AIAA SciTech 2018, Kissimmee, FL
January 10, 2018

Japan Aerospace Exploration Agency's & Kawasaki Heavy Industries' Contribution to HiLiftPW-3

Y. Ito, M. Murayama, Y. Yokokawa & K. Yamamoto (*JAXA*)
K. Tanaka & T. Hirai (*Ryoyu Systems*)
H. Yasuda (*KHI*), A. Tajima (*Kawaju Gifu Engineering*) & A. Ochi (*KHI*)

Derived from three presentations in HiLiftPW-3:

- Y. Yokokawa, Y. Ito, & M. Murayama, "JSM Experiment Overview"
- Y. Ito, M. Murayama, K. Yamamoto, K. Tanaka & T. Hirai, "TAS Code Results for the Third High Lift Prediction Workshop"
- H. Yasuda, T. Nagata, A. Tajima & A. Ochi, "KHI Contribution to HiLiftPW-3"

Outline

- Background
  - JSM Overview
  - Basic Flow Characteristics in Exp.
- Objectives
- Flow Solvers
  - TAS Code
  - Cflow
- Computational Grids
  - MEGG3D Grids
  - Cflow Grids
- Computational Results
- Concluding Remarks

JSM Overview

- **JSM** (<u>J</u>AXA High-Lift Configuration <u>S</u>tandard <u>M</u>odel)
  - Five series of wind tunnel tests in 2005 to 2009
- **Model specification**
  - 17% of assumed aircraft (100 passengers)
  - 90%-span slat
  - Inboard single- or double-slotted flap
  - Outboard single-slotted flap
  - Cylindrical fuselage
  - Pylon-mounted nacelle
  - 8 slat brackets & 3 FTFs
  - No trip dots at wind tunnel tests
- **Test facility**
  - 6.5 m x 5.5 m JAXA low-speed wind tunnel (JAXA-LWT1)
  - Closed-circuit, atmospheric pressure
  - Estimated tunnel turbulence intensity Tu = 0.16% (based on 2003 JAXA study)
- **Flow conditions**
  - M_∞ = 0.172, Re = 1.93 M, T = 33.40°C, p_{ref} = 747.70 mmHg.

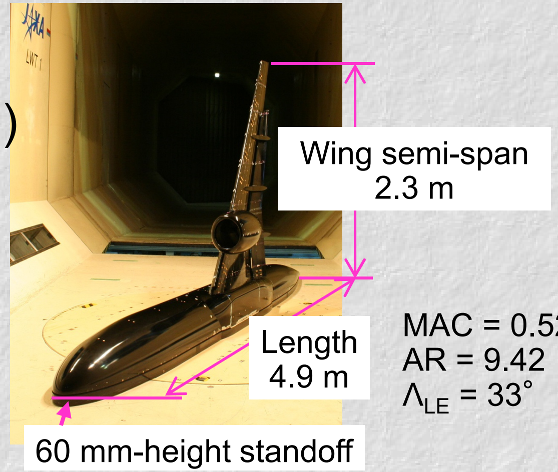

MAC = 0.529 m
AR = 9.42
Λ_{LE} = 33°

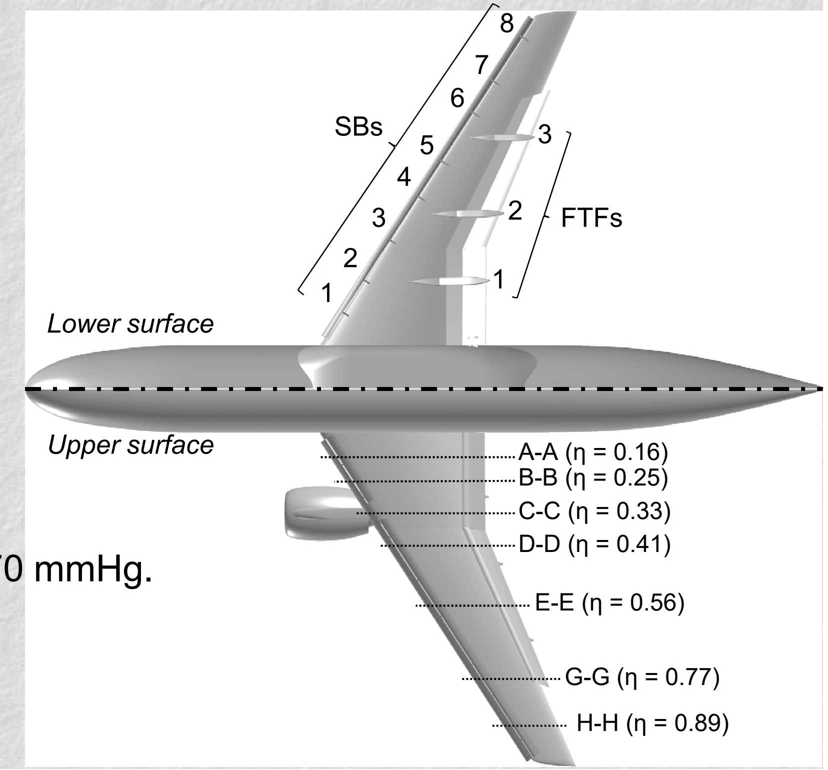

JSM Basic Flow Characteristics in Wind Tunnel α Sweep Test

- Laminar separation bubbles near the leading edge of the flap
- Flow separation in the wing tip region at high α
- Stall due to large side-of-body (SOB) separation
  - *Cf.*, Stall due to outboard wing separation by most of HiLiftPW-3 participants

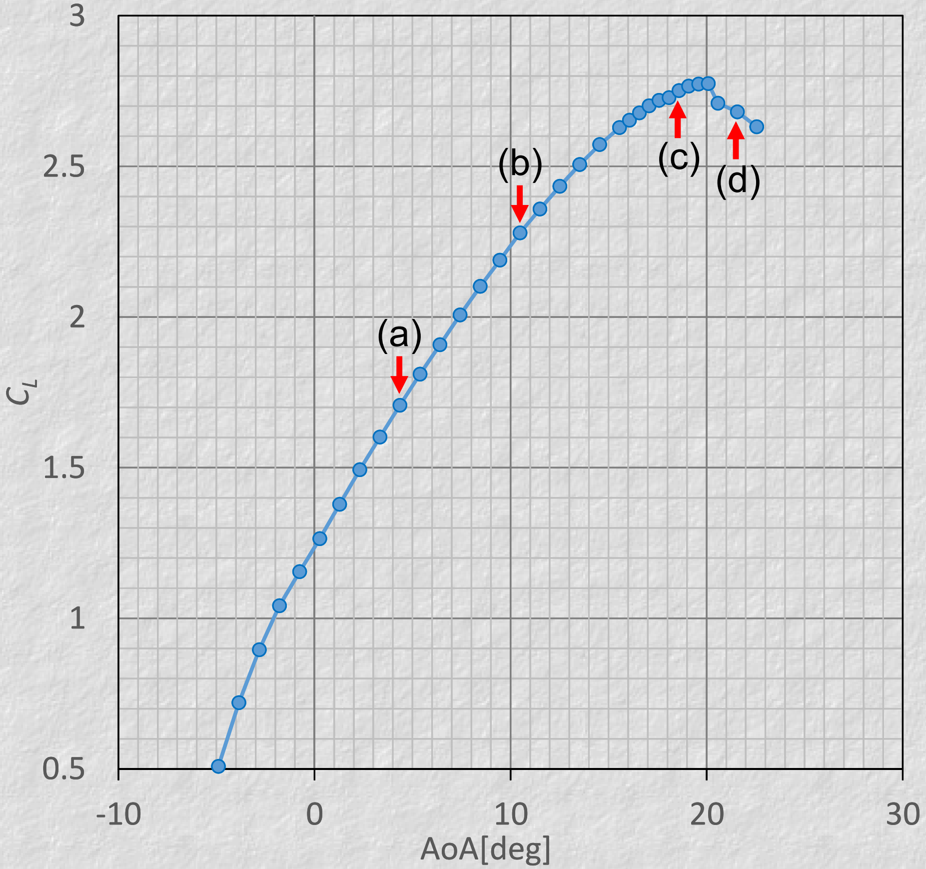

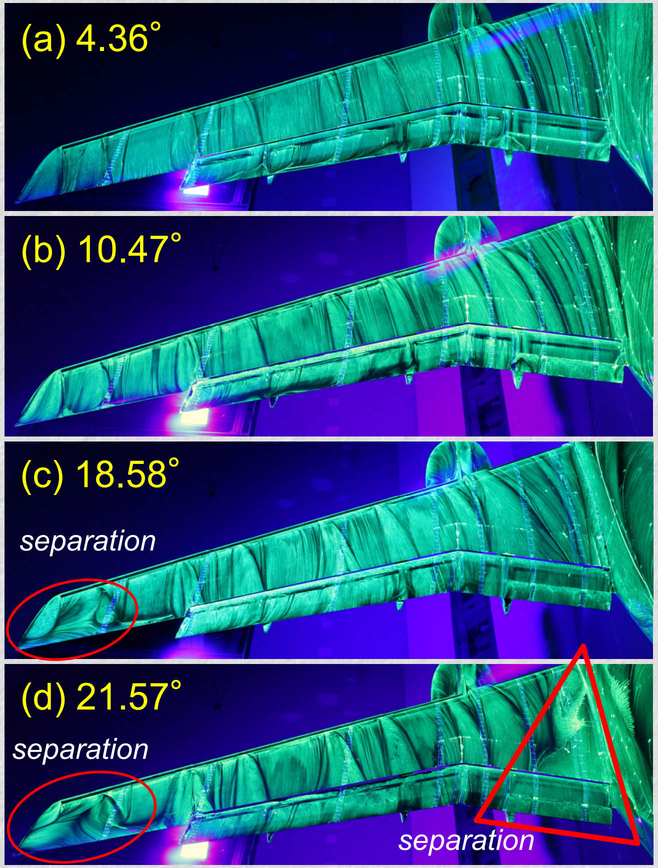

Motivation – JAXA Perspective

- Five approaches are taken to investigate differences in the prediction of the aerodynamic coefficients in CFD and experiment:
  - Effect of QCR on/off (TAS-MEGG3D)
    - Quadratic Constitutive Relation (QCR) proposed by Spalart
  - Effect of flow solvers (TAS-MEGG3D/Cflow-MEGG3D/ Cflow)
  - Effect of grid density (TAS-MEGG3D)
  - Effect of slat brackets (TAS-MEGG3D)
  - Effect of wing deformation (TAS-MEGG3D)

Motivation – KHI Perspective

- **Kawasaki Heavy Industries (KHI)** originally developed

Cflow = Grid Generator + Flow Solver

Cartesian Octree AMR
+ layered grid

Steady/Unsteady | Highly Complicated | Large Scale

- Participating AIAA workshops becomes a driving force for development, improvement and validation of CFD tools.

Aeroacoustic analyses

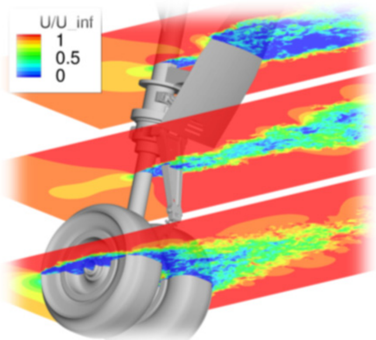

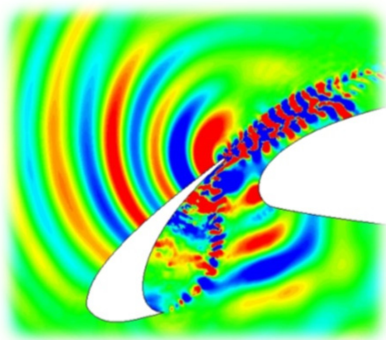

2010-2016 BANC I-IV

Aerodynamic analyses

2013 HiLiftPW-2

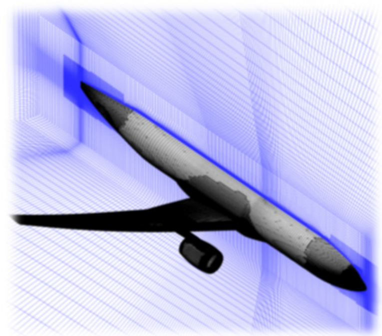

2016 DPW-6

Two Flow Solvers

- Solving full compressible Navier-Stokes equations
- Partly using similar numerical schemes:
  - MUSCL extrapolation
  - Gauss-Seidel methods for time integration
  - SA turbulence models

	TAS code (JAXA)	Cflow (KHI)
Discretization	Cell-vertex finite volume	Cell-centered finite volume
Convection flux	HLLEW 2nd-order w/ Venkatakrishnan's limiter	Simple low-dissipation AUSM scheme w/ 2nd order MUSCL method
Time integration	LU-symmetric Gauss-Seidel	Matrix free Gauss-Seidel
Turbulence model	SA-noft2-R(C_{rot}=1) & SA-noft2-R-QCR2000(C_{rot}=1)	SA-noft2

MEGG3D/Cflow Grids

JSM Grids					Solved by	
Generated by	Grid level	Config	Nodes	Elements	TAS code	Cflow
JAXA	Medium	WB	50	120	x	x
		WB w/o slat brackets	49	118	New	
		WBNP	59	139	x	x
	Fine	WB	157	384	New	
KHI	Medium	WB	164	164		x
		WBNP	181	182		x

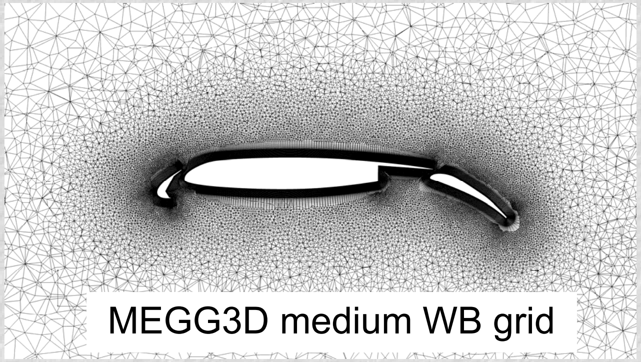

MEGG3D medium WB grid

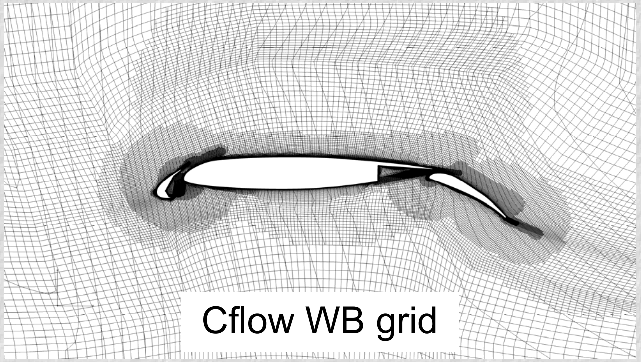

Cflow WB grid

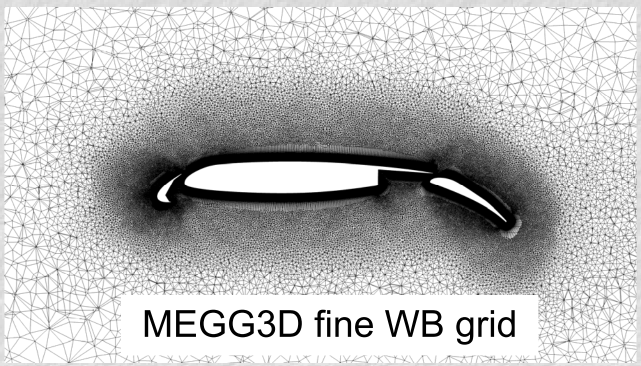

MEGG3D fine WB grid

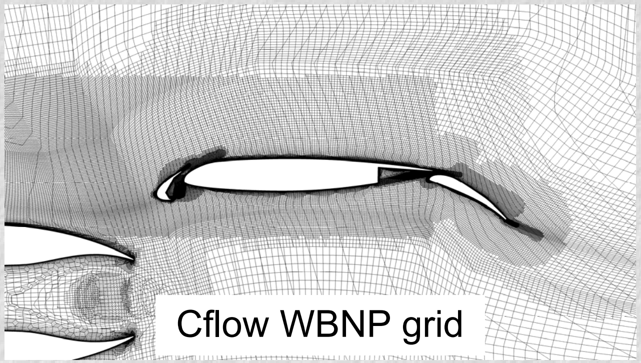

Cflow WBNP grid

MEGG3D/Cflow Grids

JSM Grids					Solved by	
Generated by	Grid level	Config	Nodes	Elements	TAS code	Cflow
JAXA	Medium	WB	50	120	x	x
		WB w/o slat brackets	49	118	New	
		WBNP	59	139	x	x
	Fine	WB	157	384	New	
KHI	Medium	WB	104	164		x
		WBNP	181	182		x

Coarser

Similar level

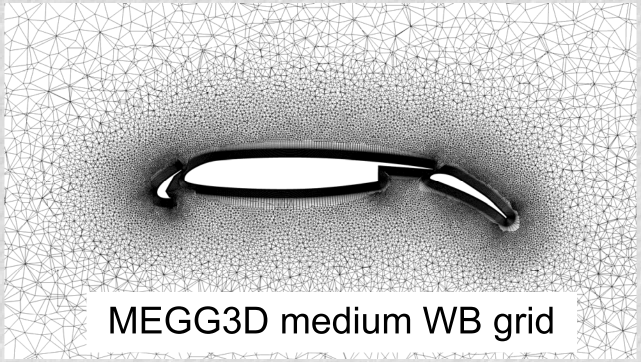
MEGG3D medium WB grid

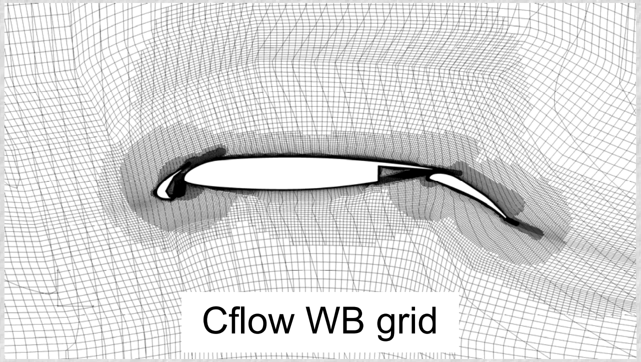
Cflow WB grid

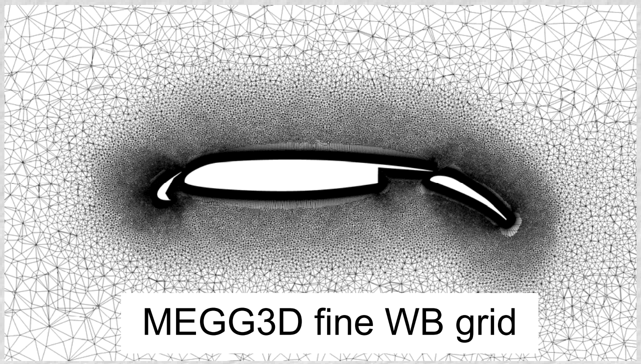
MEGG3D fine WB grid

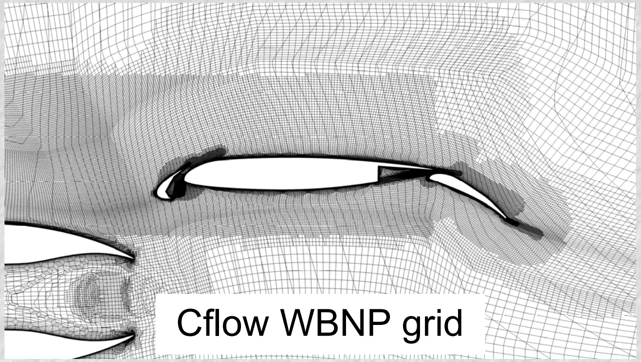
Cflow WBNP grid

MEGG3D – Mixed Element Grid Generator in 3D

- Unstructured hybrid surface/volume grid generator (prisms, hexes, tets & pyramids)
- The **Automatic Local Remeshing** enabled to reuse a volume grid generated around a baseline geometry (in this case, WB) when an additional geometry (NP) was inserted.
  - New grids were generated automatically.
  - The same elements were used except those around the additional geometry, so that its effect can be evaluated more precisely.

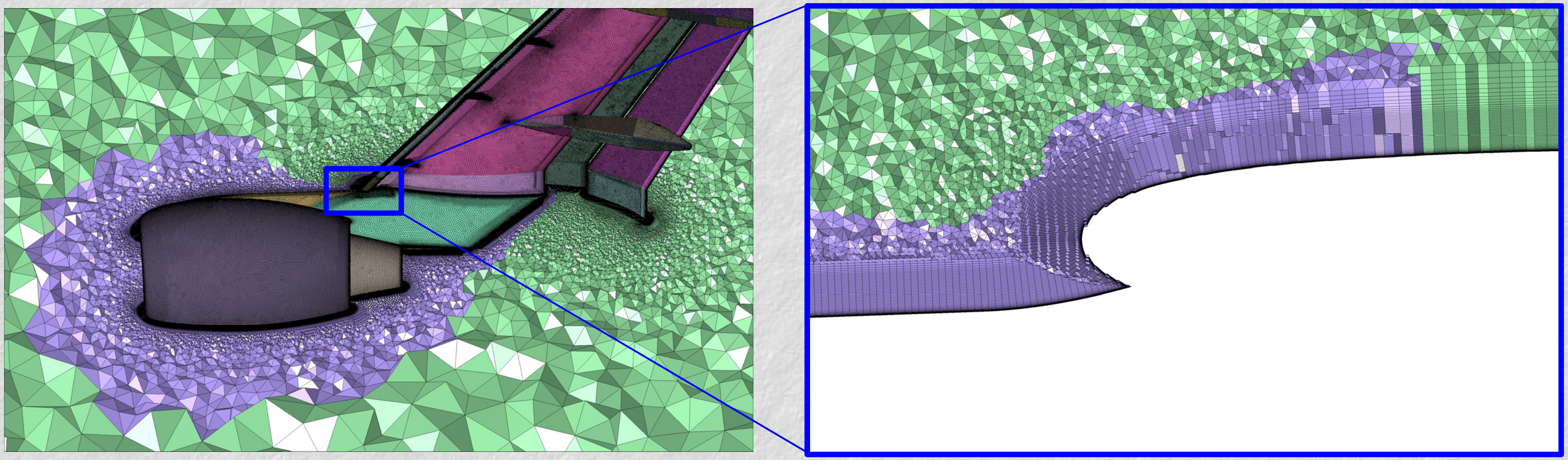

Cflow Grids

- Cflow has an **automatic Cartesian-based** grid generator **with octree adaptive grid refinement**, and **with layered grid elements on no-slip walls**.
- Cflow can generate a *NOBLU (**N**on-orthogonal **O**ctree **B**oundary-fitted **L**ayer **U**nstructured)* grid from a non-orthogonal initial grid prepared as a multi-block structured grid (no need to be body-fitted).
- The same initial grid was used for WB/WBNP configurations.

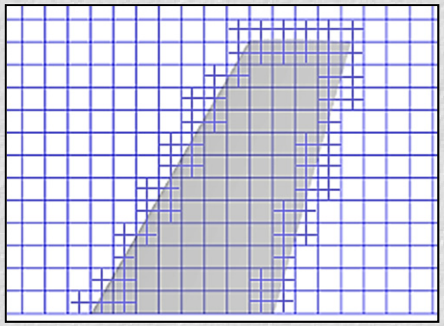

Conventional Cartesian +
1 level of octree refinement

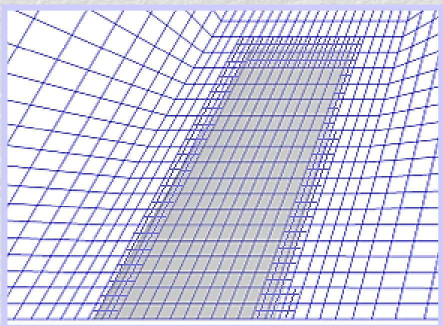

Non-orthogonal initial grid +
1 level of octree refinement

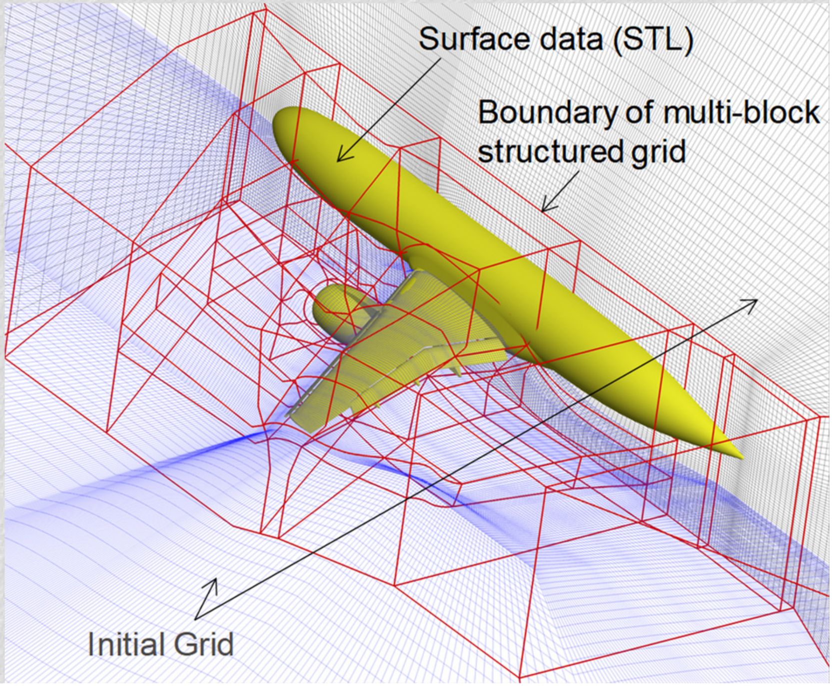

Computational Results

- **Aerodynamic coefficients**: C_L-α curves predicted by CFD will be compared with exp. in this presentation.
  - Due to the relationship between C_L and C_M.
  - Reduction in C_L → Increment in C_M
- **Surface flows**: C_f distributions on wing upper surfaces are shown in gray scale, with large flow separation areas enclosed by dashed lines.

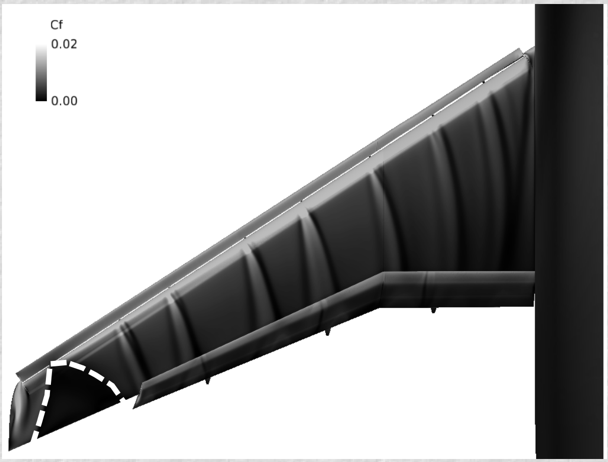

E.g., TAS code (QCR off) with MEGG3D medium grid at α = 20.59°

Effect of QCR (TAS-MEGG3D)

- Difference in C_L at high α due to larger flow separation on the outboard wing when QCR is turned on.
- For high-lift flows, the TAS code without QCR appears to be better.

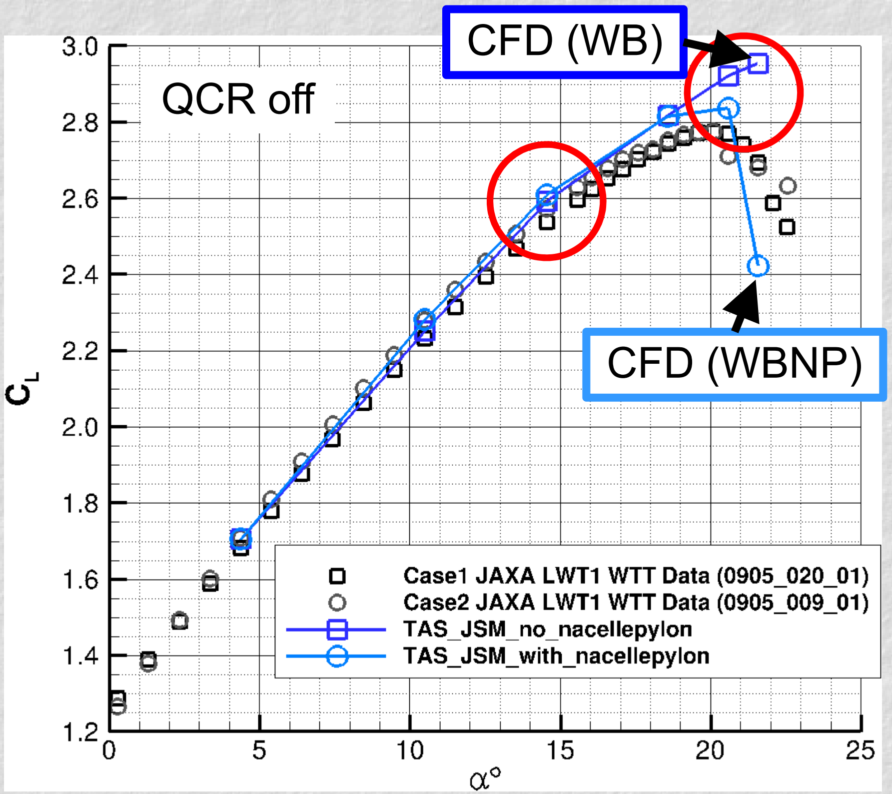

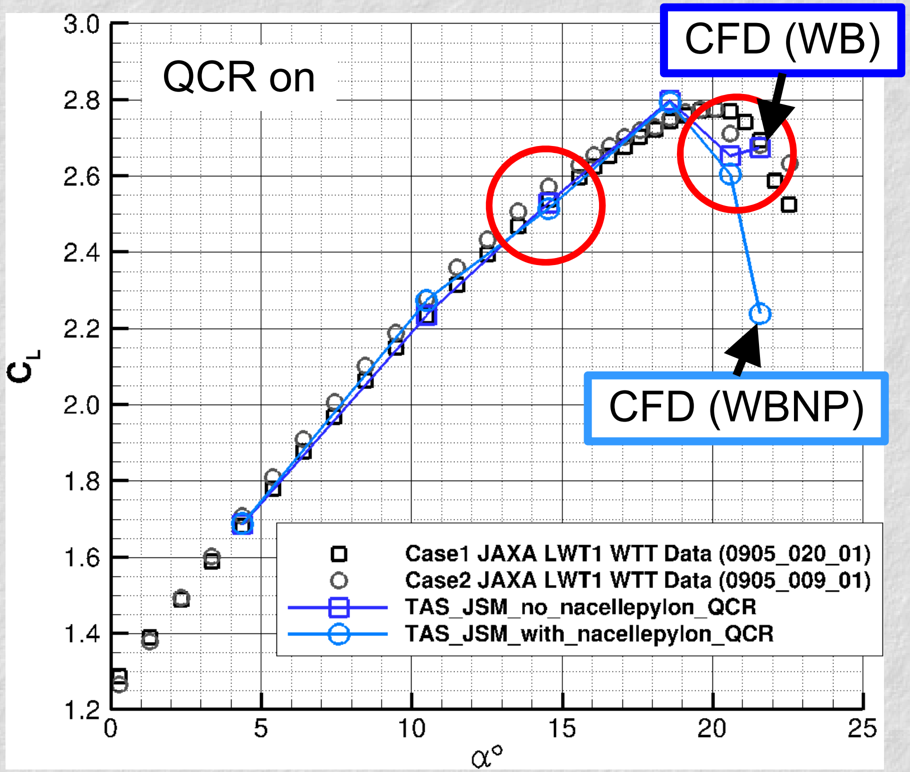

WB Config. (TAS QCR on/off)

- “QCR on” predicted larger flow separation from slat brackets.

	QCR off	QCR on
α = 14.54°	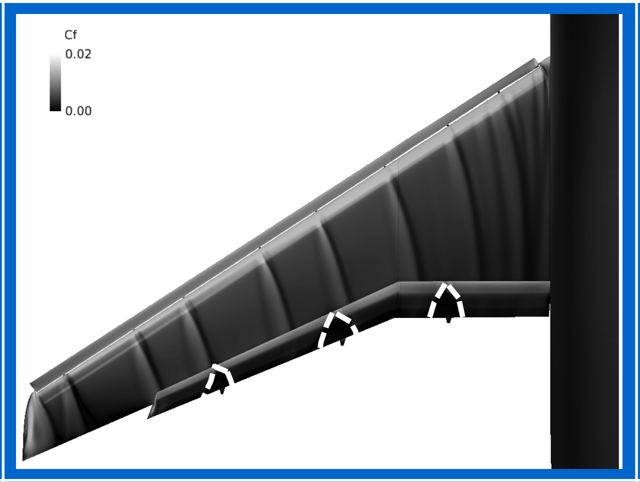	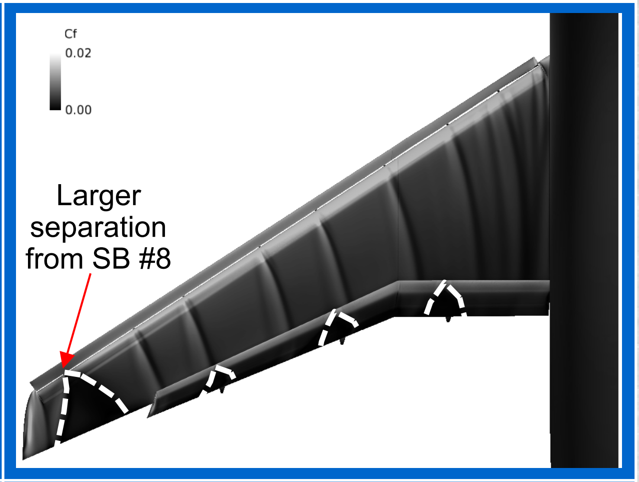
α = 20.59°		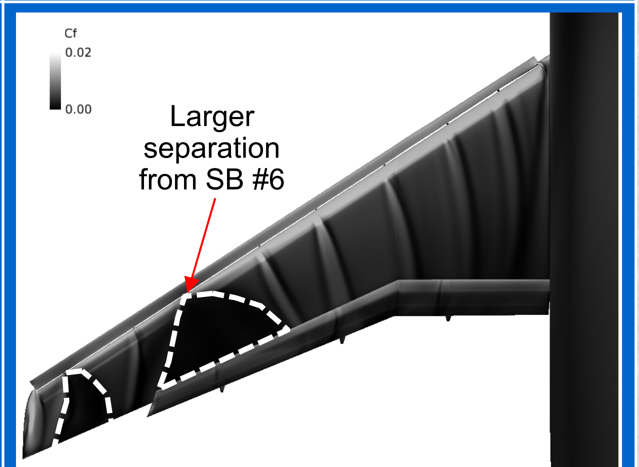

WBNP Config. (TAS QCR on/off)

<table>
<tr><th></th><th>QCR off</th><th>QCR on</th></tr>
<tr><td>α = 14.54°</td><td>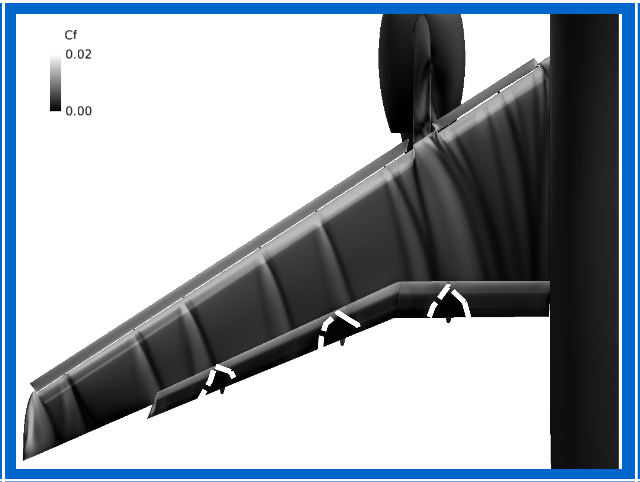
</td><td>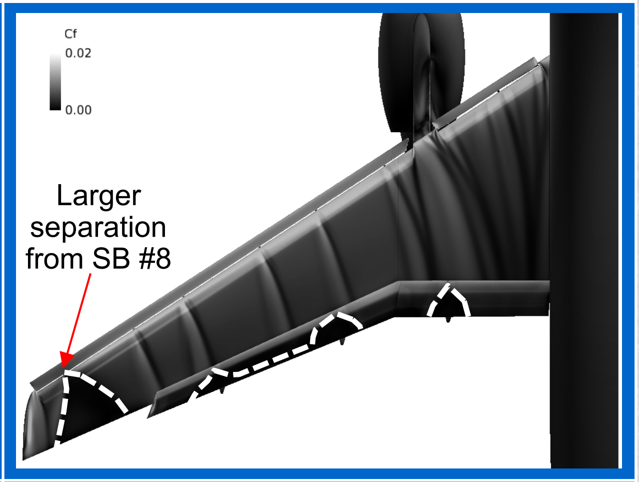
</td></tr>
<tr><td>α = 20.59°</td><td>
</td><td>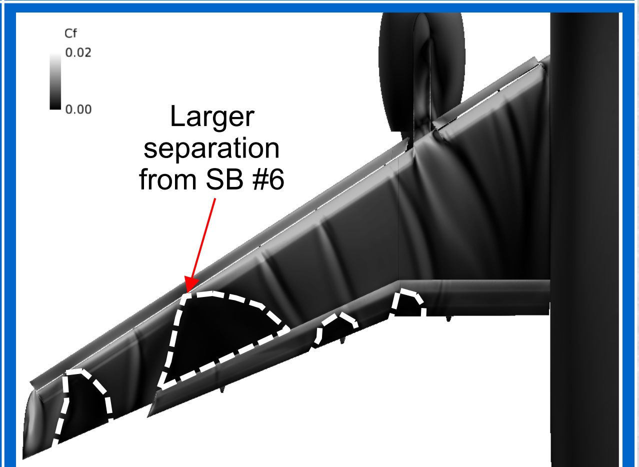
</td></tr>
</table>

SB #6 of WB Config. (TAS QCR on/off)

- "QCR on" predicted moderately weaker $\bar{p}_t$ loss at α = 20.59°, which caused the large flow separation from SB #6, or perhaps the latter caused the former in subsonic flow.

	QCR off	QCR on
α = 14.54°	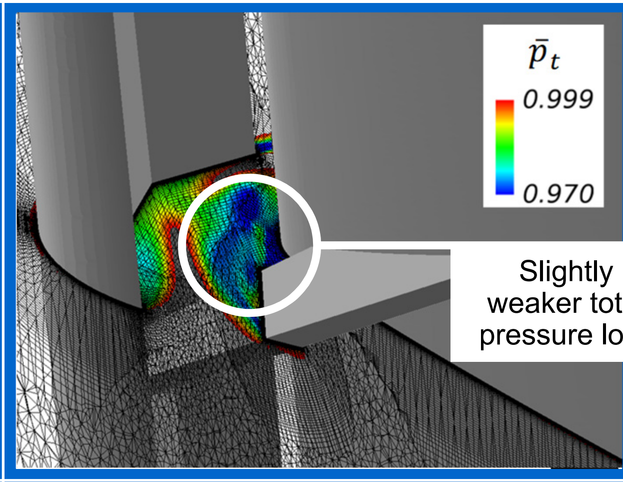	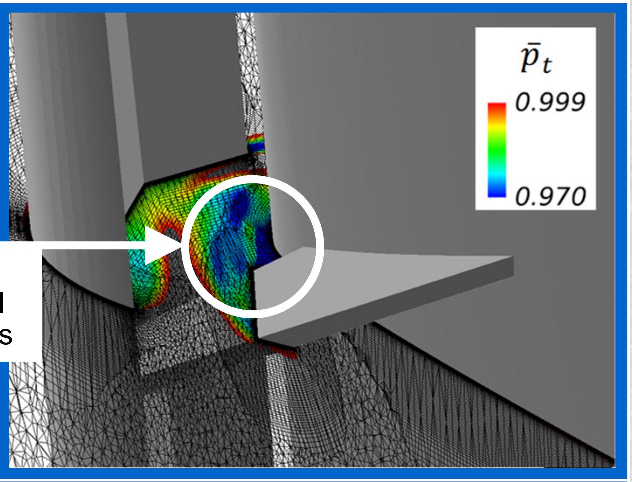
α = 20.59°	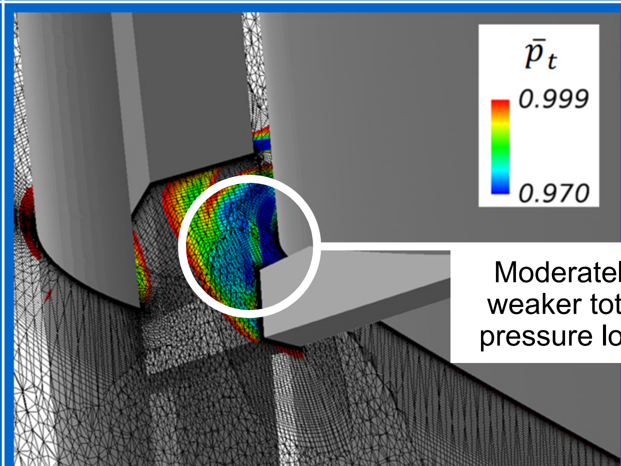	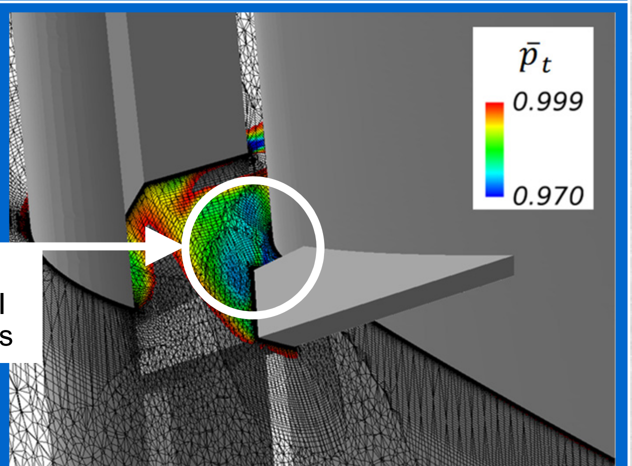

Effect of Flow Solvers (TAS-MEGG3D/Cflow-MEGG3D/Cflow)

- The nacelle installation study by CFD showed qualitatively good consistency with experiment at low α.
- Cflow predicted an earlier stall around α = 18.58° using either MEGG3D or Cflow grids.

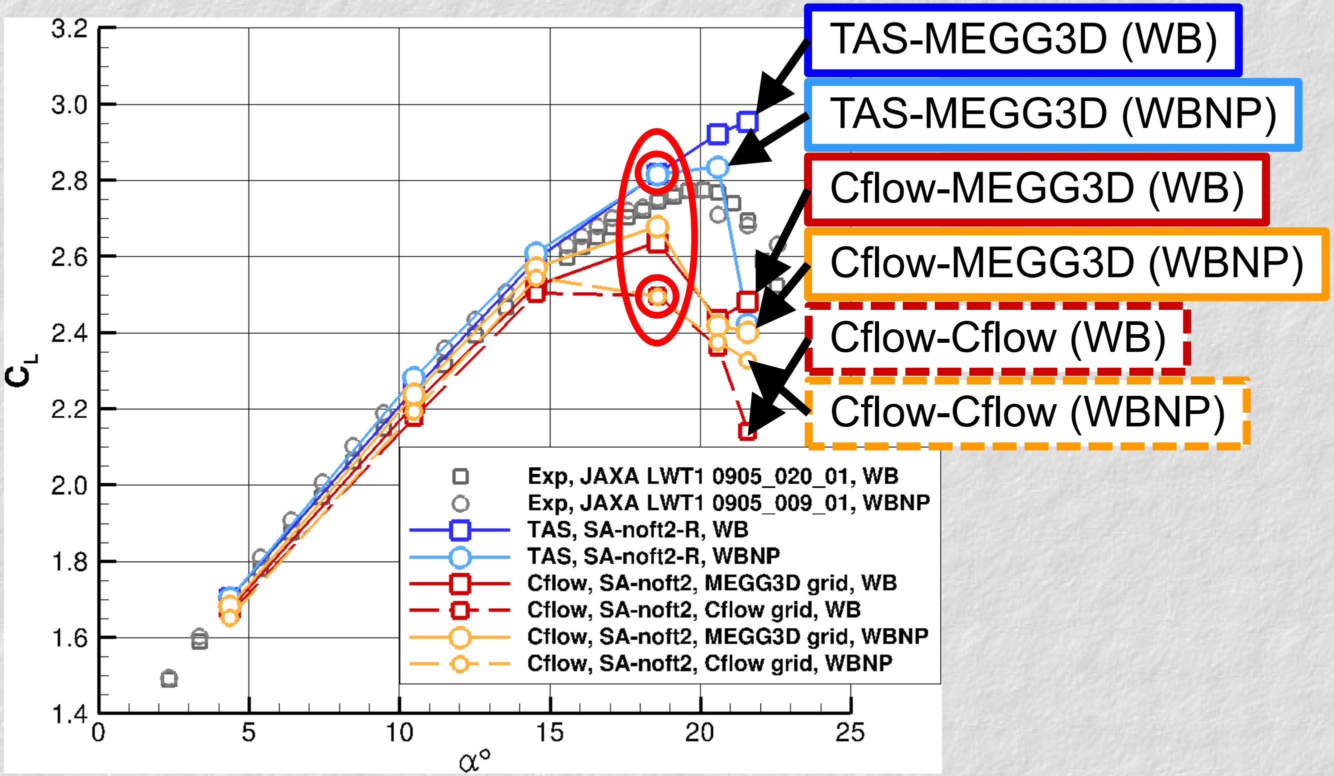

WB Config. at α = 18.58° (TAS/Cflow)

- Weaker $\bar{p}_t$ loss in the Cflow result again caused the large flow separation from SB #6.
- Partly due to the finer grid used in the Cflow simulation?

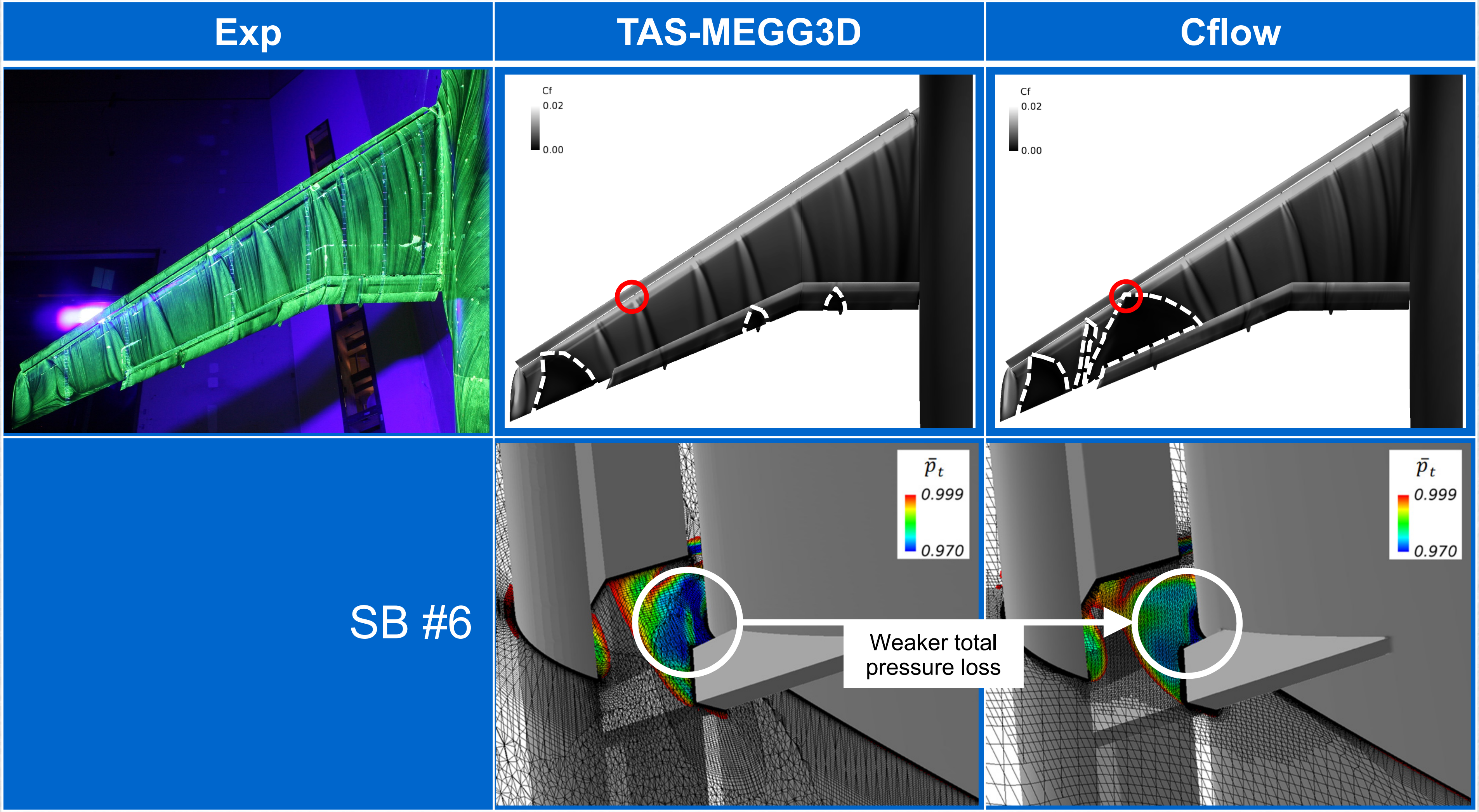

Effect of Grid Density (TAS-MEGG3D)

- The effect of grid density was investigated by the TAS code with MEGG3D medium & fine grids.
- The CFD curves match well in the range of 10.47° < α < 21.57°.
- The smaller C_L with the fine grid is due to slightly larger flow separation on the flap.
- The fine grid predicted a stall before α = 21.57°.

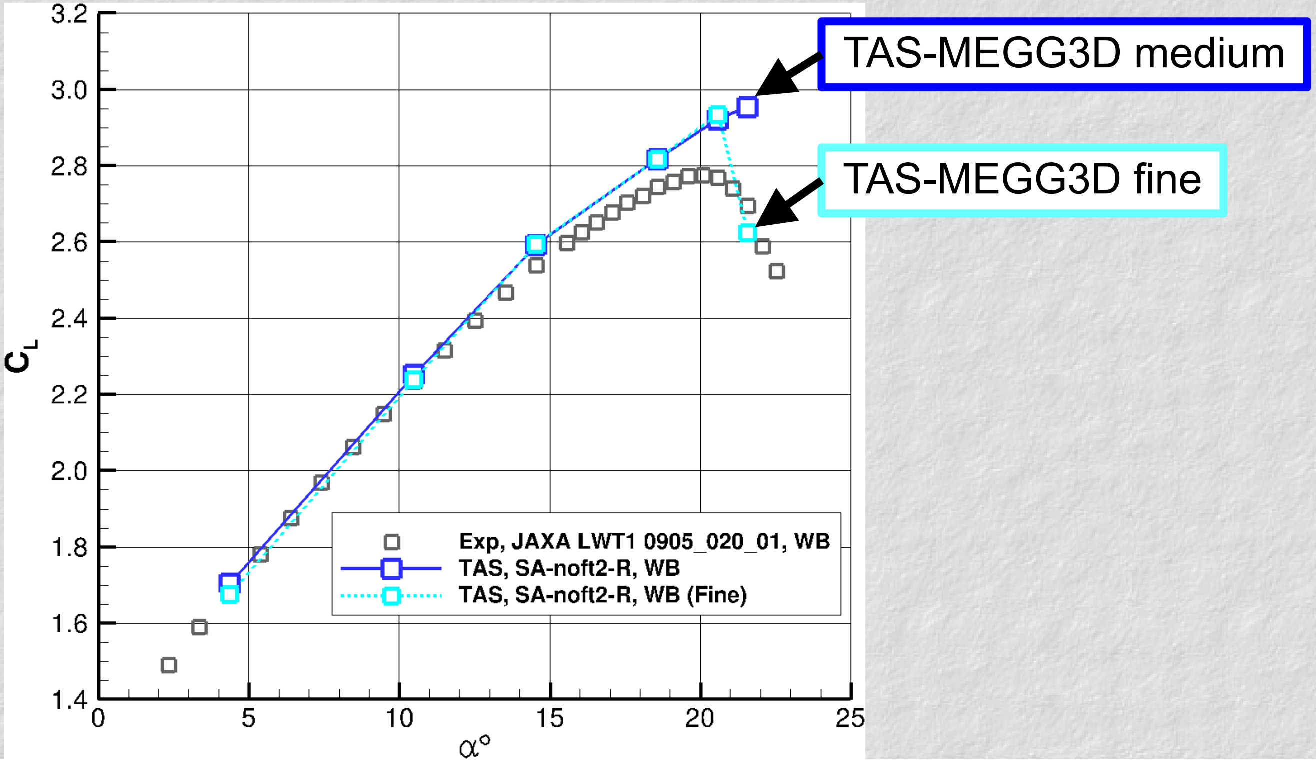

WB Config. at α = 21.57° (TAS-MEGG3D)

- The fine grid predicted large flow separation from SB #5.

Exp	MEGG3D medium	MEGG3D fine

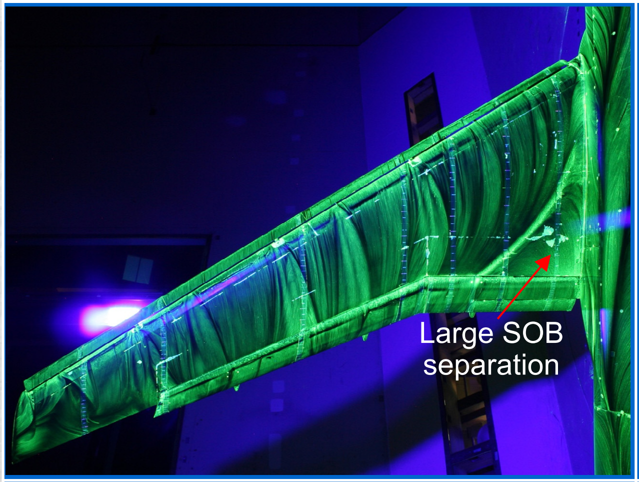

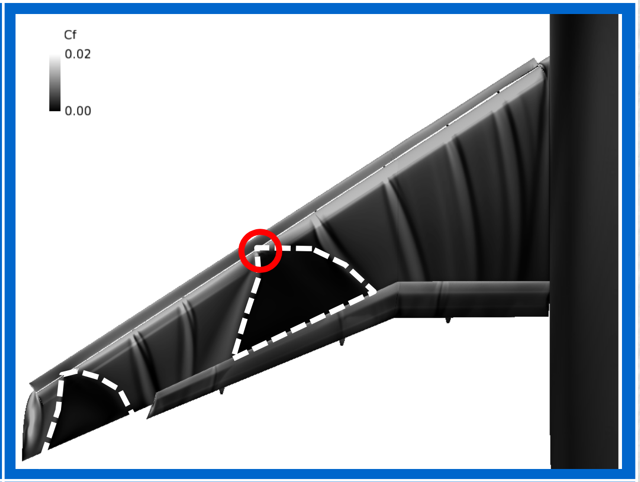

SB #5

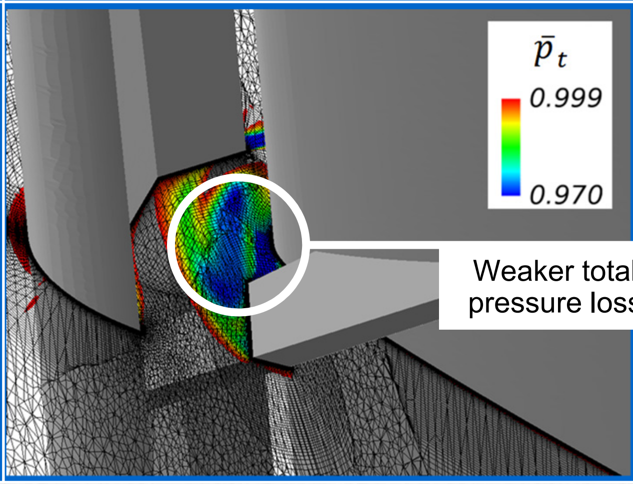

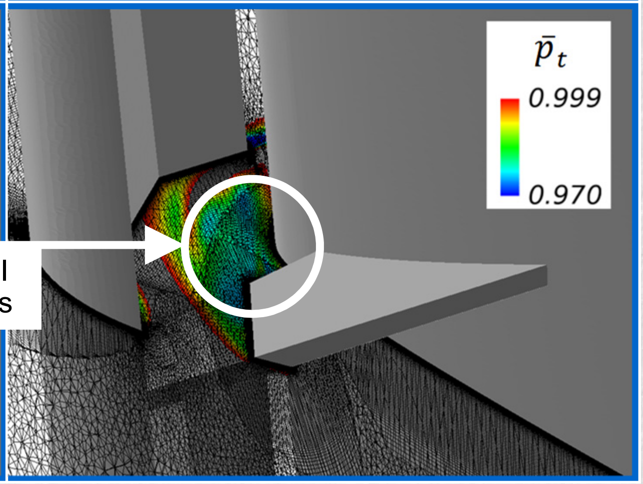

Effect of Slat Brackets (TAS-MEGG3D)

- For the WB config. w/o SBs, the TAS code predicted
  - Higher C_L due to the reduction of flow separation on the outboard wing.
  - Stall due to SOB flow separation, agreed with exp.

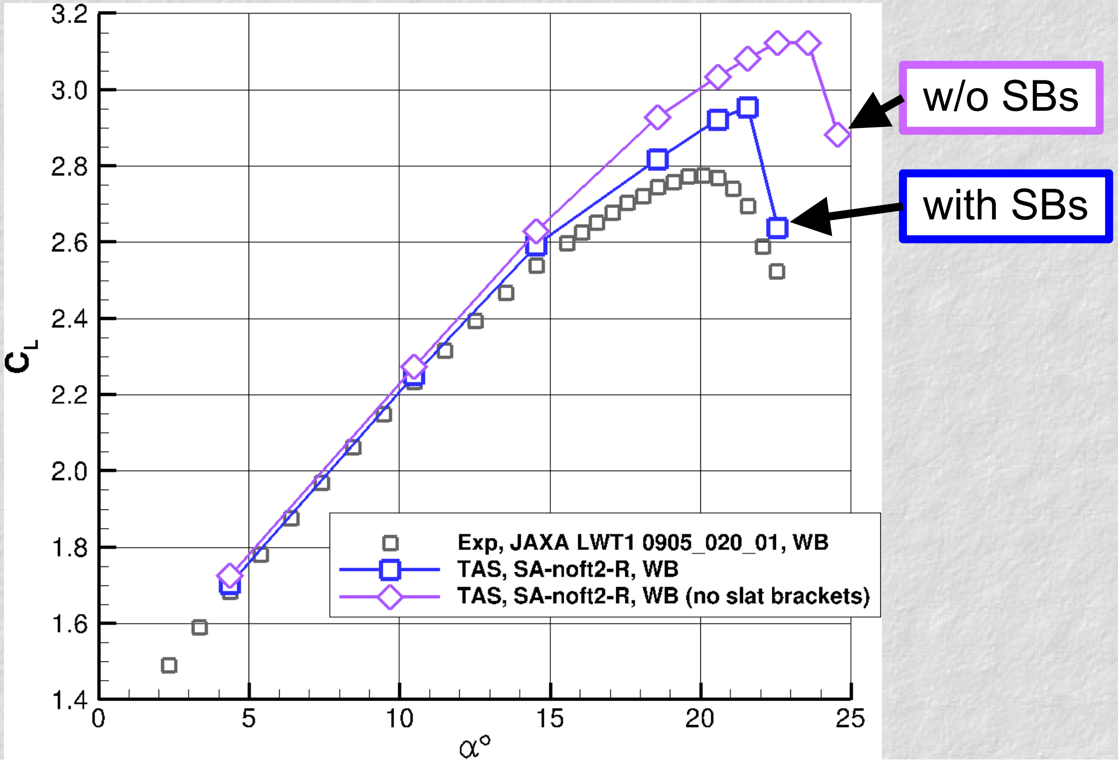

WB Config. with & w/o SBs at α ≥ 18.58° (TAS-MEGG3D)

- W/o SBs, stall is caused by SOB separation. Flow separation occurs on the flap even at high α, but the lift generated at the flap is similar to the case with SBs.

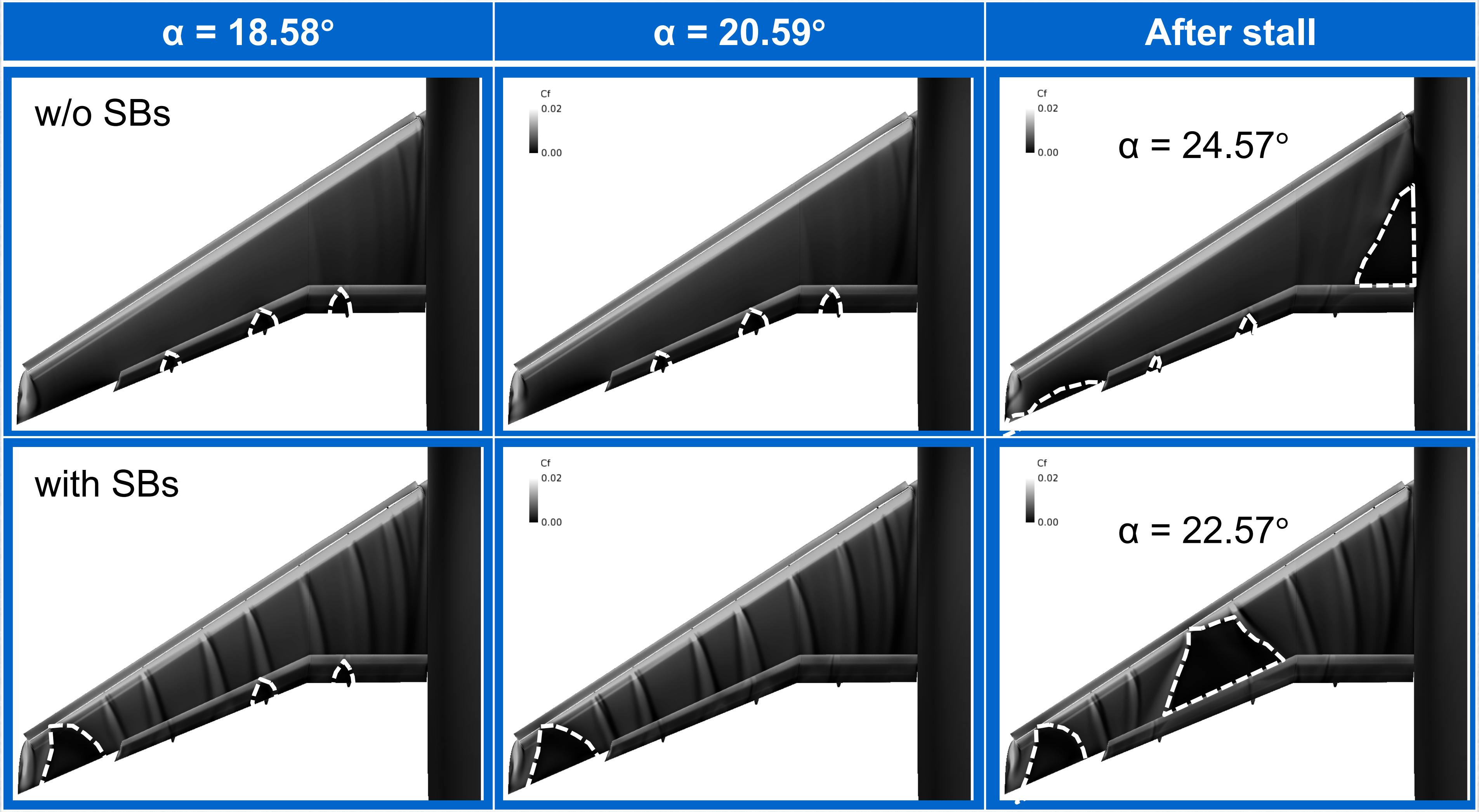

Wing Deformation

- Quartic polynomial was approximated using displacement data at 32 markers on the main wing in exp. to estimate wing bending & twisting.
  - Gap, overlap and deflection angle of the slat & flap were not changed.
- For CAD models, 10 sections defined on the wing reference plane were deformed using shape morphing of CATIA V5.
  - Distributed for public use
- For volume grids, the same polynomial was used for the surfaces, and interior nodes were moved accordingly.
  - Currently, WB configuration at α = 20° only.

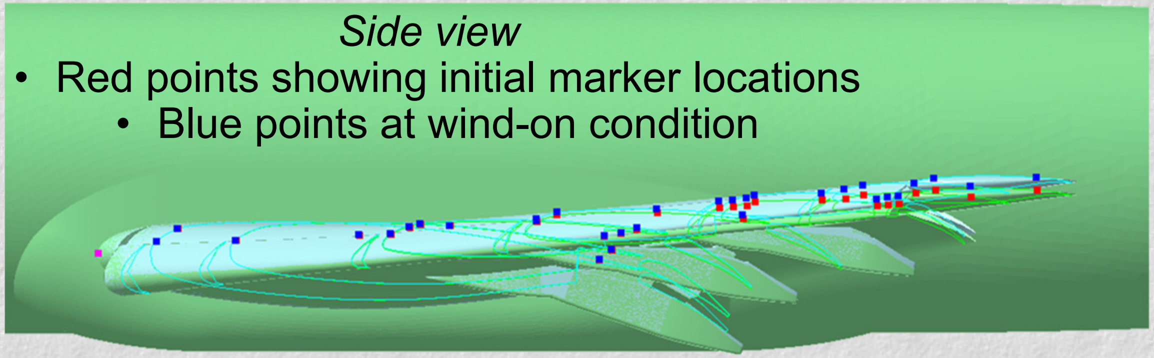

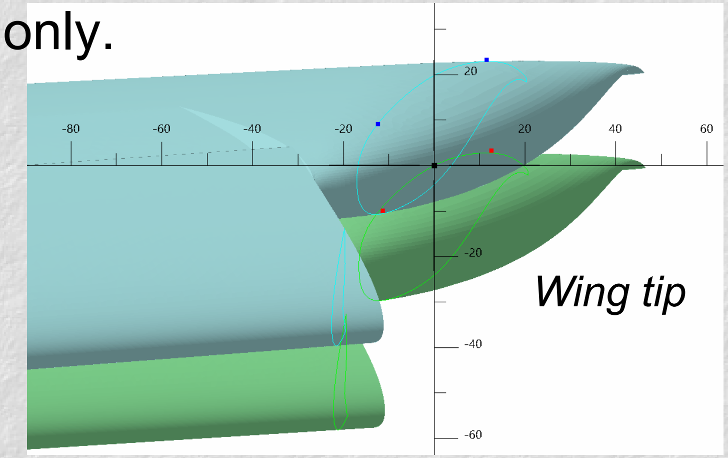

Effect of Wing Deformation (TAS-MEGG3D)

- No significant effects of the geometry change were observed in the aerodynamic coefficients and flow fields.

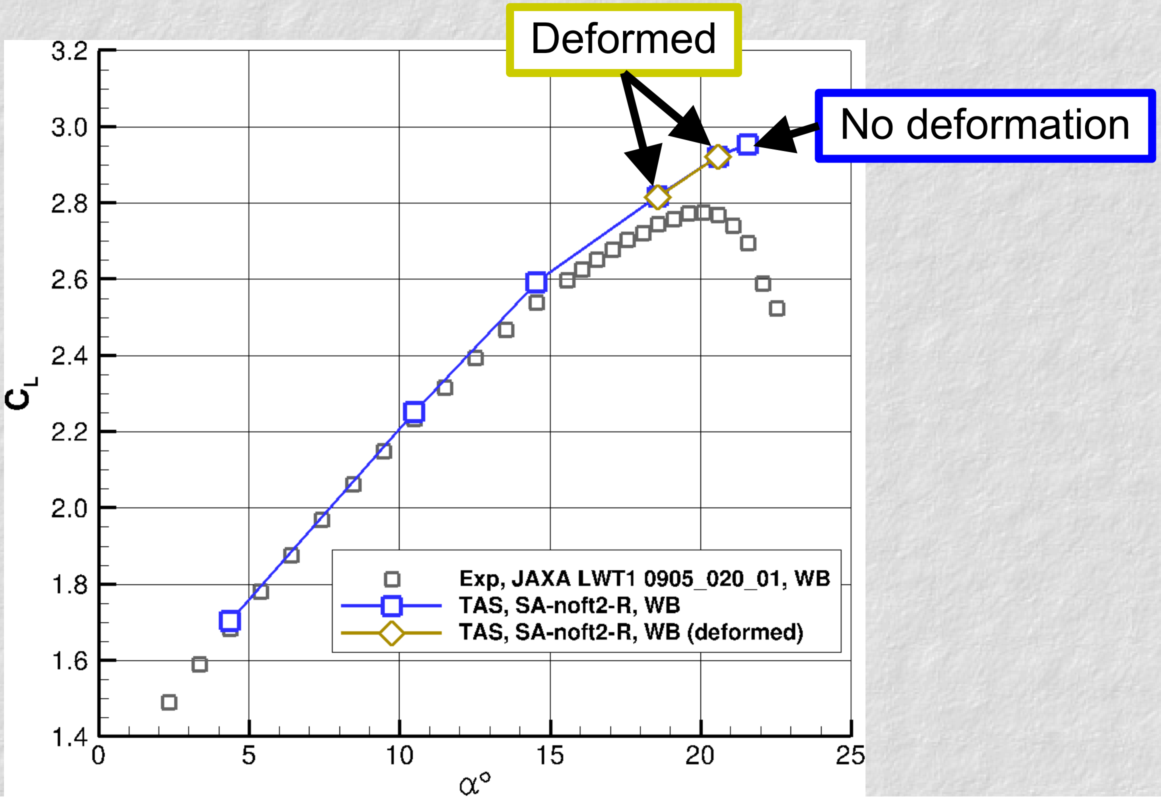

C_p Distributions & Surface Streamlines

- The size of the flow separation is similar at each α.

	No deformation	Deformed
α = 18.58°	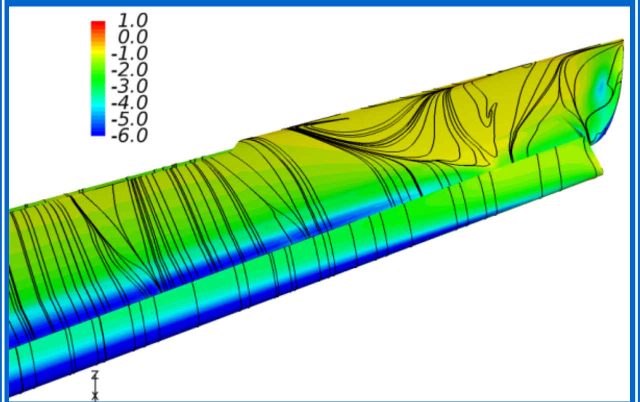	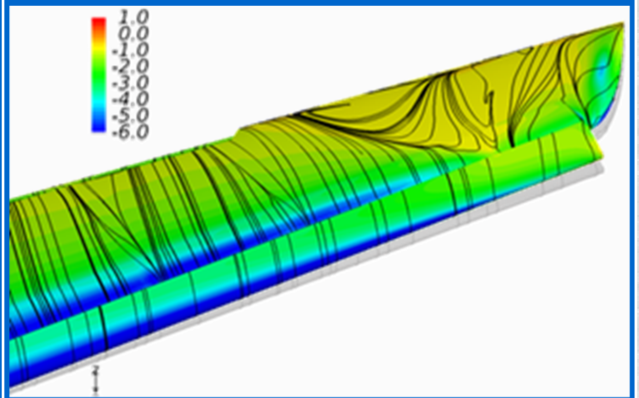
α = 20.59°	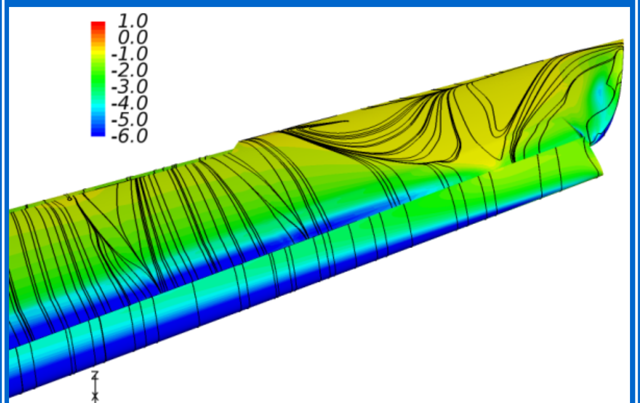	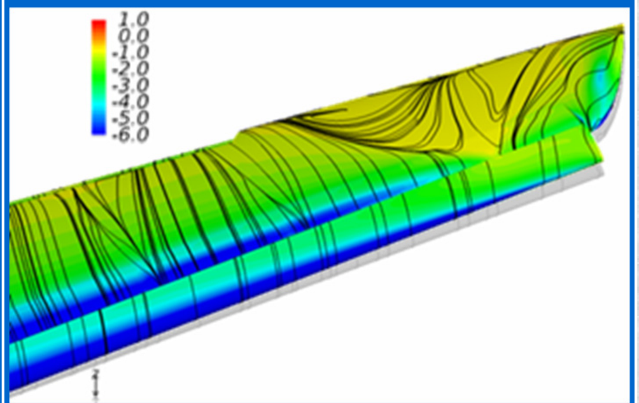

Concluding Remarks

- JAXA contributed its JSM WB and WBNP configs and wind tunnel test data to HiLiftPW-3 as one of the test cases for a nacelle installation study.
- The nacelle installation study by the TAS code and Cflow showed qualitatively good consistency with wind tunnel test results for C_L, C_D and C_M at low α.
- Five approaches were taken to investigate the reason why the JSM stall mechanism mainly due to the SOB separation found in the experiment was not predicted by HiLiftPW-3 participants:
  - Effect of QCR on/off
  - Effect of flow solvers
  - Effect of grid density
  - Effect of slat brackets
  - Effect of wing deformation
- CFD results revealed a relationship between the $\bar{p}_t$ loss around the slat brackets and the prevention of flow separation on the main wing.
- The SOB separation that caused the stall in the wind tunnel test was not predicted by either the TAS code or Cflow.
  - Stall due to SOB separation for the WB config. w/o SBs by the TAS code.
- Continuous investigations with finer grids and on the selection of initial conditions at high α are needed as future works.